EUROPEAN LABORATORY FOR PARTICLE PHYSICS

Status report to the proposal P330

Report from the NA61/SHINE experiment at the CERN SPS

By the NA61 Collaboration
http://na61.web.cern.ch

CERN-SPSC-2011-035 / SPSC-SR-091
18/10/2011

Abstract

This document reports on the status and plans of the NA61/SHINE experiment at the CERN SPS as of October 2011. First, progress on detector upgrades and overviews of the 2010 and 2011 data taking periods are presented. The NA61 facility is ready for data taking with ion beams. Second, the advance in the NA61 software, data calibration and the data analysis is reported. In particular, first NA61/SHINE charged pion spectra in $p+\mathrm{C}$ interactions at 31 GeV/c were recently published. Here we also present preliminary results on K^+ spectra. Both data sets have already been used for improving the neutrino beam flux predictions in the T2K experiment. Third, new results from LHC and RHIC relevant for the NA49 evidence of the onset of deconfinement are reviewed and their impact on the NA61 ion program is discussed. Finally, plans for data taking in 2012, 2014 and 2015 are outlined in view of the scheduled stop of the CERN accelerators in 2013.

Recent developments underline the urgency of carrying out the NA61/SHINE ion program as soon as technically possible. In particular, the most urgent data for this program, central Ar + Ca collisions at 13A, 20A, 30A, 40A, 80A and 158A GeV/c should be taken with as little delay as possible. It is also crucial to complete the energy scan with secondary Be beams in 2011 and 2012.

Contents

The NA61/SHINE Collaboration

N. Abgrall[22], A. Aduszkiewicz[23], T. Anticic[13], N. Antoniou[18], J. Argyriades[22], B. Baatar[9], A. Blondel[22], J. Blumer[5], M. Bogusz[24], A. Bravar[22], W. Brooks[1], J. Brzychczyk[8], A. Bubak[12] S. A. Bunyatov[9], O. Busygina[6], T. Cetner[24], P. Christakoglou[18], P. Chung[16], T. Czopowicz[24], N. Davis[18], S. Debieux[22], F. Diakonos[18], S. Di Luise[2], W. Dominik[23], J. Dumarchez[11], R. Engel[5], A. Ereditato[20], L. Esposito[2], G. A. Feofilov[15], Z. Fodor[10], A. Ferrero[22], A. Fulop[10], M. Gaździcki[17,21], M. Golubeva[6], B. Grabez[26], K. Grebieszkow[24], A. Grzeszczuk[12], F. Guber[6], H. Hakobyan[1], T. Hasegawa[7], R. Idczak[25], S. Igolkin[15], Y. Ivanov[1], A. Ivashkin[6], K. Kadija[13], A. Kapoyannis[18], N. Katrynska[25], D. Kielczewska[23], D. Kikola[24], M. Kirejczyk[23], J. Kisiel[12], T. Kiss[10], S. Kleinfelder[28], T. Kobayashi[7], O. Kochebina[15], V. I. Kolesnikov[9], D. Kolev[4], V. P. Kondratiev[15], A. Korzenev[22], S. Kowalski[12], A. Krasnoperov[9], S. Kuleshov[1], A. Kurepin[6], R. Lacey[16], D. Larsen[19], A. Laszlo[10], V. V. Lyubushkin[9], M. Maćkowiak-Pawłowska[21], Z. Majka[8], A. I. Malakhov[9], D. Maletic[26], A. Marchionni[2], A. Marcinek[8], I. Maris[5] V. Marin[6], K. Marton[10], T. Matulewicz[23], V. Matveev[6,9], G. L. Melkumov[9], M. Messina[20], St. Mrówczyński[17], S. Murphy[22], T. Nakadaira[7], K. Nishikawa[7], T. Palczewski[14], G. Palla[10], A. D. Panagiotou[18], T. Paul[27], W. Peryt[24], O. Petukhov[6] R. Planeta[8], J. Pluta[24], B. A. Popov[9,11], M. Posiadala[23], S. Puławski[12], J. Puzovic[26], W. Rauch[3], M. Ravonel[22], R. Renfordt[21], A. Robert[11], D. Röhrich[19], E. Rondio[14], B. Rossi[20], M. Roth[5], A. Rubbia[2], A. Rustamov[21], M. Rybczynski[17], A. Sadovsky[6], K. Sakashita[7], T. Sekiguchi[7], P. Seyboth[17], M. Shibata[7], R. Sipos[10], A. N. Sissakian[9,*], E. Skrzypczak[23], M. Slodkowski[24], P. Staszel[8], G. Stefanek[17], J. Stepaniak[14], H. Stroebele[21], T. Susa[13], M. Szuba[5], M. Tada[7], A. Taranenko[16], V. Tereshchenko[9], T. Tolyhi[10], R. Tsenov[4], L. Turko[25], R. Ulrich[5], M. Unger[5], M. Vassiliou[18], D. Veberic[27], V. V. Vechernin[15], G. Vesztergombi[10], A. Wilczek[12], Z. Wlodarczyk[17], A. Wojtaszek[17], O. Wyszyński[8], L. Zambelli[11], W. Zipper[12]

[1]Universidad Tecnica Federico Santa Maria, Valparaiso, Chile
[2]ETH, Zurich, Switzerland
[3]Fachhochschule Frankfurt, Frankfurt, Germany
[4]Faculty of Physics, University of Sofia, Sofia, Bulgaria
[5]Karlsruhe Institute of Technology, Karlsruhe, Germany
[6]Institute for Nuclear Research, Moscow, Russia
[7]Institute for Particle and Nuclear Studies, KEK, Tsukuba, Japan
[8]Jagiellonian University, Cracow, Poland
[9]Joint Institute for Nuclear Research, Dubna, Russia
[10]KFKI Research Institute for Particle and Nuclear Physics, Budapest, Hungary
[11]LPNHE, University of Paris VI and VII, Paris, France
[12]University of Silesia, Katowice, Poland
[13]Rudjer Boskovic Institute, Zagreb, Croatia
[14]Soltan Institute for Nuclear Studies, Warsaw, Poland
[15]St. Petersburg State University, St. Petersburg, Russia
[16]State University of New York, Stony Brook, USA
[17]Jan Kochanowski University in Kielce, Poland
[18]University of Athens, Athens, Greece
[19]University of Bergen, Bergen, Norway
[20]University of Bern, Bern, Switzerland
[21]University of Frankfurt, Frankfurt, Germany
[22]University of Geneva, Geneva, Switzerland
[23]Faculty of Physics, University of Warsaw, Warsaw, Poland
[24]Warsaw University of Technology, Warsaw, Poland
[25]University of Wrocław, Wrocław, Poland
[26]University of Belgrade, Belgrade, Serbia
[27]Laboratory of Astroparticle Physics, University Nova Gorica, Nova Gorica, Slovenia
[28]University of California, Irvine, USA
* *deceased*

1 Introduction

This NA61 annual report presents briefly the status and plans of the NA61/SHINE experiment at the CERN SPS [1]. The report refers to the period October 2010 – October 2011.

The document is organized as follows. Detector upgrades are listed in Section 2. An overview of the 2010 test of secondary ion beams and of the 2011 data taking period until October 2011 is given in Sections 3 and 4. Progress in software and calibration as well as the status of the data analysis is presented in Sections 5 and 6, respectively. New results from LHC and RHIC relevant for the NA49 evidence of the onset of deconfinement are reviewed and their impact on the NA61 ion program is discussed in Section 7. Finally, plans for data taking in 2012, 2014 and 2015 are outlined in Section 8. The list of publications and conference contributions is given in the Appendix.

2 Detector upgrades

Progress in the basic detector upgrades over the last year is reported below. The upgrades, mainly needed for data taking with ion beams starting in November 2011 (the PSD and Z-detectors, the He beam pipes) as well as data taking on $p+$Pb interactions starting in 2012 (the LMPD detector), are completed. The NA61 facility is well prepared for runs with ion beams.

2.1 Projectile Spectator Detector (PSD)

The search for the critical point of strongly interacting matter in relativistic nucleus-nucleus collisions requires precise control over fluctuations in the number of interacting nucleons. In NA61/SHINE the number of interacting projectile nucleons will be determined by measurements of the number of non-interacting nucleons from the projectile nuclei (the number of projectile spectators). These measurements will be done by a very forward hadron calorimeter called the Projectile Spectator Detector (PSD). Basic design requirements of the PSD are a good energy resolution and a high transverse uniformity necessary for the determination of the number of spectators with a precision of one nucleon.

The PSD is a modular lead/scintillator sandwich calorimeter with fine transverse and longitudinal segmentation. Light collection is provided by WLS-fibers embedded in the scintillator plates and light readout by compact micro-pixel avalanche photo-diodes (MAPDs). The complete PSD calorimeter consists of 44 modules which cover a transverse area of $120 \times 120\,\mathrm{cm}^2$, see Fig. 1 left.

The central part of the PSD consists of 16 small modules with transverse dimension of $10{\times}10\,\mathrm{cm}^2$ and weight 120 kg each. The outer part of the PSD comprises 28 large $20{\times}20\,\mathrm{cm}^2$ modules with a weight of 500 kg each. The production of 16 small and 16 large modules needed for the 2011 Be run was finished in summer 2011. All these modules were assembled in an array on the movable PSD platform, see Fig. 1 right. Front-End-Electronics as well as

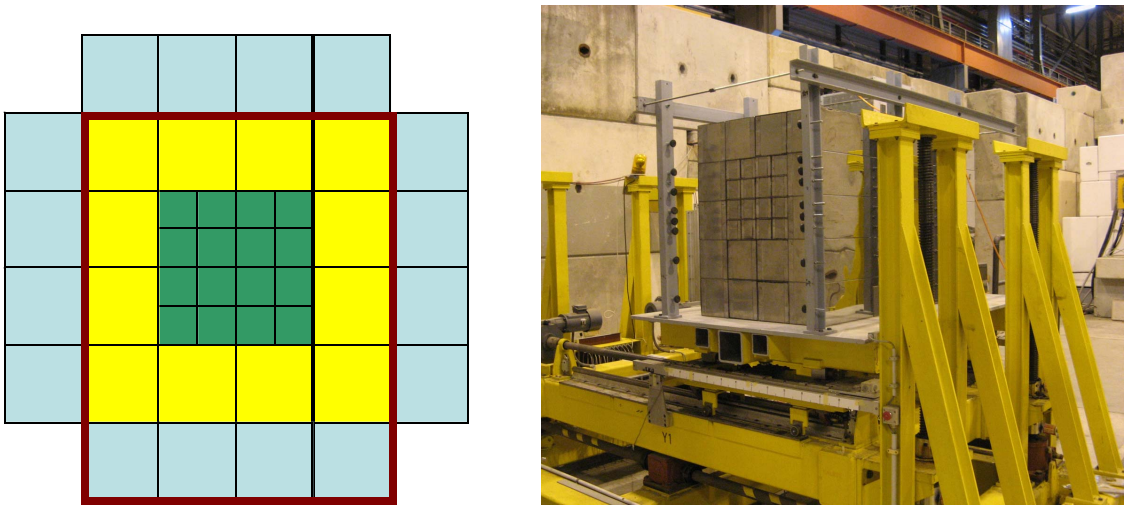

Figure 1: *Left:* Schematic front view of the PSD structure. Red lines mark the constructed and installed parts of the calorimeter. *Right:* Photo of the PSD calorimeter installed on the movable platform.

the data readout are ready and tested for all 44 modules. The remaining 12 large modules will be assembled by the end of 2011. Commissioning and calibration of the assembled array of 32 modules was carried out during the physics run in September 2011 using the 158 GeV/c proton beam. Analysis of the collected calibration data is in progress. The PSD calorimeter with 32 modules is ready for the first NA61 ion run in November–December 2011.

2.2 Z-detectors

In order to achieve good charge identification of secondary ions delivered to NA61, Quartz and Gas Cherenkov counters will be used.

- The Quartz detector with a 2.5 mm thick quartz radiator is equipped with two photomultipliers (X2020Q) attached to both sides of the quartz plate, see Fig. 2 left. Optical grease (BC630) is applied between the PMTs and the quartz plate in order to achieve good light transition.

- The Gas detector uses a 60 cm long C4F10 gas radiator. The construction of this detector is based on the standard CERN threshold Cherenkov unit. Cherenkov photons are reflected by a 25 μm thick aluminized mylar foil and focused by a parabolic mirror onto a single photomultiplier, Hamamatsu R2059.

Both detectors were tested during the 2011 proton run.

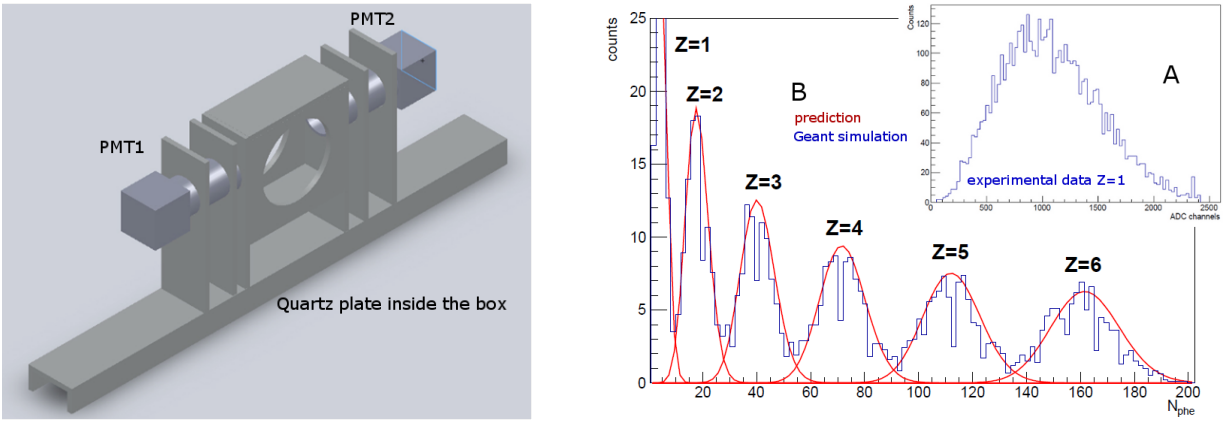

Figure 2: *Left:* The schematic view of the Quartz Z-detector. *Right:* The spectrum of photo-electrons for nuclei with $Z = 1$ to 6 charges is shown for the data-based prediction (solid red line) and for the Geant4 simulation (histogram). The inset shows the ADC spectrum measured during the Quartz Z-detector test with proton beam at 158 GeV/c in 2011.

The experimental ADC distribution measured by the Quartz detector for particles with $Z = 1$ is presented in Fig. 2 right. Based on the experimental data the mean value of photo-electrons for $Z = 1$ particles, before any amplification, was estimated to be 4.5. Figure 3 shows a comparison between the Geant4 simulation and the prediction based on the data. The resolution is about $\sigma(Z) \approx 0.27$ in the region of Be ions.

For the Gas Cherenkov detector the experimental ADC distribution for the measured charge was fitted with a Poisson distribution to extract the number of primary photo–electrons, the blue line in Fig. 3. The noise imposed on the signal was assumed to be at the level of 20%. Under this condition the estimated mean value of the photo-electrons is about 31. The model predictions of the detector response for $Z = 4$, 5, and 6 are presented in Fig. 3. The estimated resolution in ion charge will be about $\sigma(Z) \approx 0.11$ in the region of Be ions. This was calculated under the assumption that the noise for $Z = 4$ is larger by factor of 3 than the noise estimated for protons (red line).

2.3 *A*-detector

The A-detector was constructed for the 2010 test run with secondary ion beams. Its primary goal is to determine the mass composition of the secondary ion beam by precise time of flight measurements. The detector was installed at a distance of about 140 m upstream of the NA61 target, see Fig. 4 left.

The A-detector consists of a plastic scintillator bar $150 \times 5 \times 15\,\mathrm{mm}^3$ with light readout from both ends by two fast Russian FEU-187 PMTs. The achieved time resolution of about 100 ps is enough to separate boron ions ^{10}B and ^{11}B up to beam momentum of about $15A$ GeV/c. For the 2011 and 2012 ion runs a new A-detector with the same scintillator

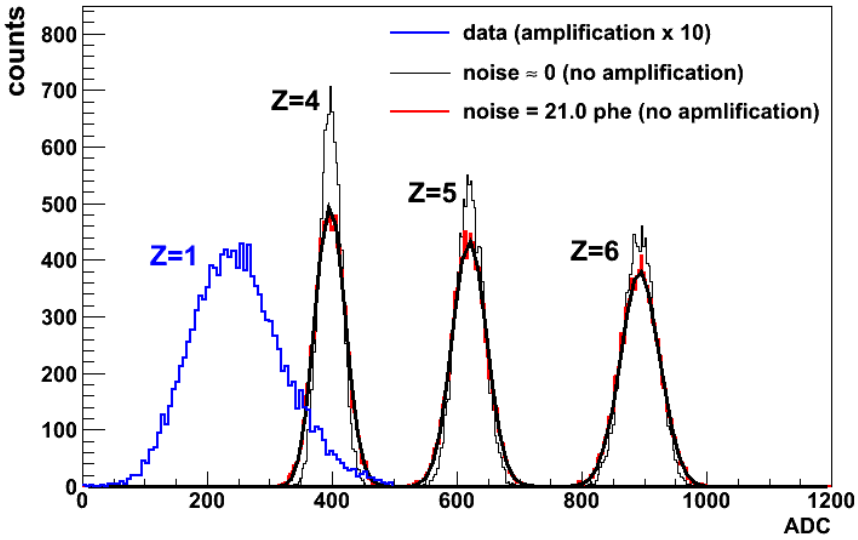

Figure 3: The experimental ADC distribution and the model predictions of the Gas Cherenkov detector response for $Z = 4$, 5, and 6.

but improved mechanical support structure was constructed. The FEU-187 PMTs were replaced by the $\langle 96 \rangle$ EMI 9133 type. The new A-detector was tested in the PS T10 beam line in September 2011, see Fig. 4 right.

2.4 Low Momentum Particle Detector (LMPD)

In hadron–nucleus interactions the collision centrality can be determined by the number of emitted low momentum protons (the so-called *grey protons*). For this purpose a special detector, the Low Momentum Particle Detector (LMPD), was developed. The detector consists of two small size TPC chambers on the two sides of the target with a vertical drift field, and a sequence of detection layers picking up the ionization signal of radially emitted particles. Between the detection layers plastic absorber layers are inserted. Therefore the range of particles can be determined in the absorber material. The range and ionization response of a particle depends on its energy and particle type, and therefore event-by-event counting of the number of emitted low energy protons becomes possible. Prototypes of the detector were tested in 2009 and 2010.

The final version of the LMPD, see Fig, 5, was manufactured in 2011, and was first tested in the NA61 experimental area, downstream of the NA61 detector, in parasitic mode. The tests showed the expected performance of the detector, namely its capability of proton identification and of counting the low energy (grey) protons. A typical reconstructed event with its clusters and tracks is seen in Fig. 6 left, whereas the ionization response of particles with fixed range is shown in Fig. 6 right. The broad peak corresponds to the signal of protons with a selected range.

The main operational parameters of the LMPD were optimized during the 2011 test

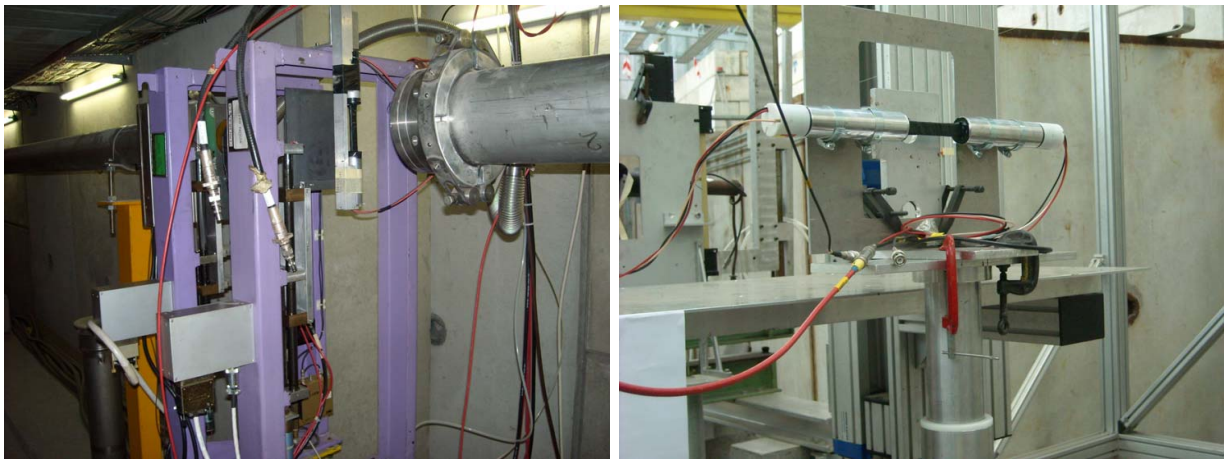

Figure 4: The A-detector installed in the SPS H2 beam line in the December 2010 test run (left). Test of the new A-detector in the PS T10 beam line in September 2011 (right).

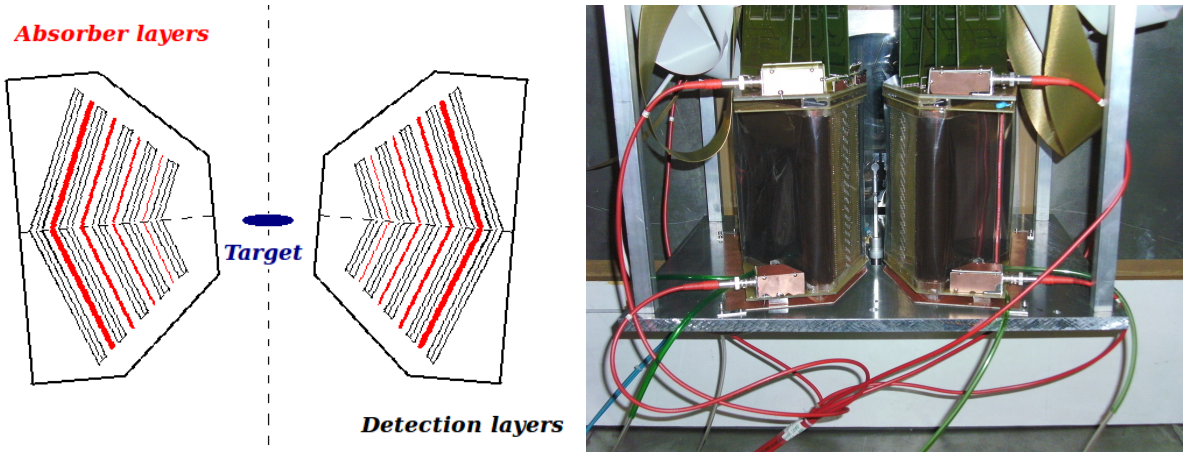

Figure 5: *Left:* Schematic top view of the LMPD. Red lines indicate the absorber layers. Each absorber layer is placed between sensitive layers in order to determine whether a given particle from the target traversed the absorber layer or stopped inside the absorber. *Right:* Photo of the LMPD detector from the direction of the beam at the NA61 target position. The Pb target (in the middle), and the field cage strips (copper strips on capton) are well visible. Conventional NA61 TPC Front End electronics were used for readout (on top).

operation. In particular, a gradual decrease of amplification in the layers close to the target was introduced. This is necessary in order to adjust the dynamical range for the expected high ionization particles. After optimization, large statistics physics-quality data were recorded, still in the downstream position of NA61 in parasitic mode. They allow for systematic study of the gray proton production and absorption in the target material. During the last 3 days of the 2011 NA61 158 GeV/c $p+p$ run, the LMPD was mounted

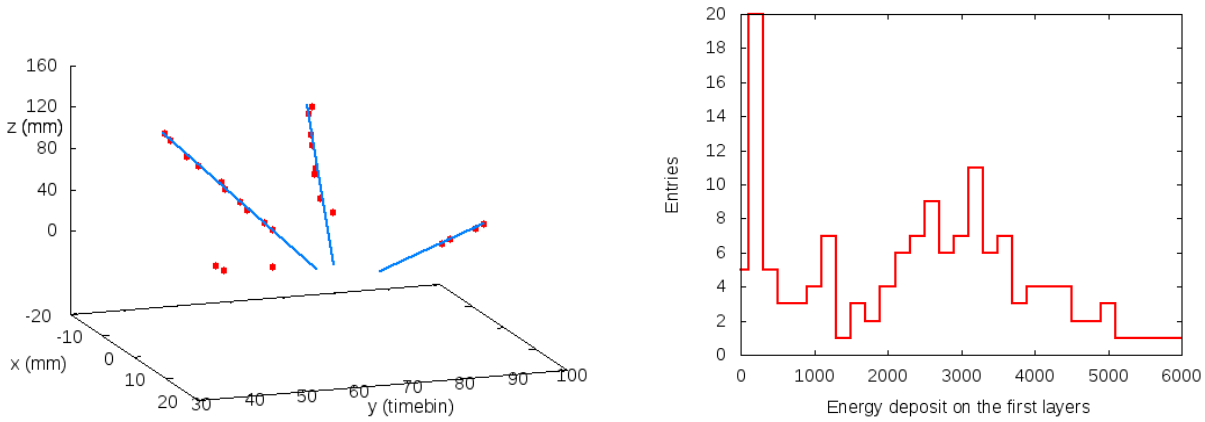

Figure 6: *Left:* Tracks reconstructed form signals registered by a single LMPD wedge from a typical p + Pb interaction at 158 GeV/c. Red points indicate the position of the reconstructed clusters in the local detector coordinate system, blue lines depict the straight particle tracks fitted to them. The particle tracks point to a common production vertex within the target. *Right:* Energy deposit of particles traversing the first absorber, but stopped within the second absorber layer. The wide peak in the middle corresponds to the expected response of protons.

in the normal target position of NA61, and preliminary physics-quality p + Pb data were recorded with the LMPD integrated into the full NA61 detector. This ensures the smooth start-up of the large statistics 158 GeV/c p + Pb run of NA61, planned for 2012. The data recorded with LMPD in 2011 are listed in Table 1.

Beam	**Target**	**Detector setup**	**Num. of events**
p at 158 GeV/c	0.5 mm Pb foil	Standalone test beam setup	2.4 M
p at 158 GeV/c	0.5 mm Pb foil at 45°	Standalone test beam setup	600 k
p at 158 GeV/c	2.0 mm C foil	Standalone test beam setup	550 k
p at 158 GeV/c	1.0 mm Al foil	Standalone test beam setup	620 k
p at 158 GeV/c	2.0 mm Pb foil	Physics setup with full NA61	700 k
p at 158 GeV/c	0.5 mm Pb foil	Physics setup with full NA61	400 k

Table 1: The recorded number of physics-quality events in various configurations during the LMPD test and pilot physics data taking for p + Pb collisions at 158 GeV/c in 2011. Recording of these data was preceded by tests of the chamber, alignment runs, and runs for finding optimal values of the main operational parameters.

2.5 He beam pipes

The He beam pipes were installed in March/April 2011 in the gas volume of the NA61 Vertex TPCs in order to reduce the number of δ-electrons by a factor of about 10. This is needed in order to decrease significantly event-by-event fluctuations of the track density in the TPCs and thus reduce systematic uncertainties of fluctuation measurements in nucleus-nucleus collisions. Installation of the pipe necessitated cutting openings in the double wall mylar envelopes of VTPC-1 and VTPC-2. The openings were drilled using specially developed tools which prevented dust and debris of material from getting into the inner volume of the TPCs. These openings into the gas volume were precisely positioned around the beam axis and were used for gluing the lightweight interface units (200 μm wall thickness carbon fiber rings) providing support for the He beam pipe and ensuring a hermetic VTPC volume.

The lightest possible He beam-pipe structure was produced that is feasible with present technology. The close-to-normal gas pressure conditions allow to use thin (30 μm) gas-leakage tight Tedlar [2] polyvinyl fluoride (PVF) film to produce 2.5 m length cylinder envelopes (pipes of 75 and 96 mm diameters), which formed the He gas and protective gas volumes. The pipes were made by gluing the Tedlar film to special rigid, extremely light-weight carbon fiber end-caps strengthened with Airex foam [3]. This provides low-mass beam pipe fixation, separation of gases and hermetic sealing. Use of light-weight low-Z materials allows to minimize the probability of secondary interaction processes. They include:

- Tedlar polyvinyl fluoride (PVF) film [2],
- Carbon Fiber M55J, $\rho = 1.92\,\mathrm{g/cm^3}$, $X_0 = 25\,\mathrm{cm}$,
- Toray [4] and
- Airex foam, $\rho = 0.03\,\mathrm{g/cm^3}$, $X_0 = 1390\,\mathrm{cm}$ [3].

The construction is gas tight allowing perfect separation of helium used in the central pipe from the working gas of the TPC. During the operation an inert gas (preferably CO_2) is flushed through the outer envelope of the pipe (the protective gas volume).

The He pipe installed in the Vertex TPC, with gas supply lines connected, is shown in Fig. 7 left. A special gas supply system was constructed to maintain the overpressure gradient in the pipe with respect to the pressure in the TPC. This is mandatory to assure the mechanical stability of the pipes.

The He pipes were tested under working conditions of the Vertex TPCs. They showed good mechanical stability when operating different modes of gas circulation in the TPCs. No leakage of helium from the central pipe to the outer envelope was observed. The surface of the pipe did not show any excessive charging-up which could distort the drift field in the active TPC volume. Gas tightness of the fixations of the pipes to the mylar foils closing the VTPC field cage was tested by monitoring of the oxygen content in the TPC gas. The oxygen contamination of the working gas decreased to a few ppms during the first 48 hours

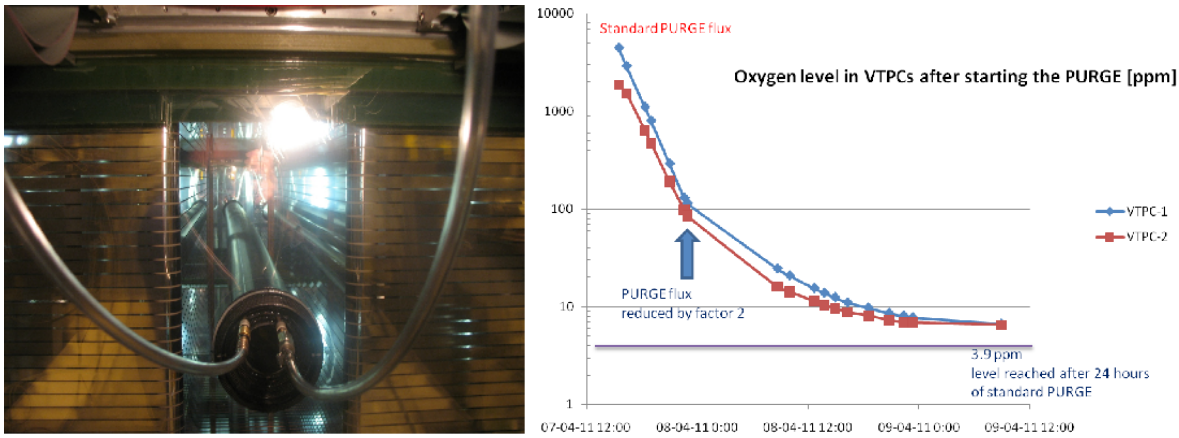

Figure 7: *Left:* The He beam pipe installed in the VTPC-1 gas-volume between the two field cages. *Right:* Oxygen level in the VTPC volumes during the gas purging period.

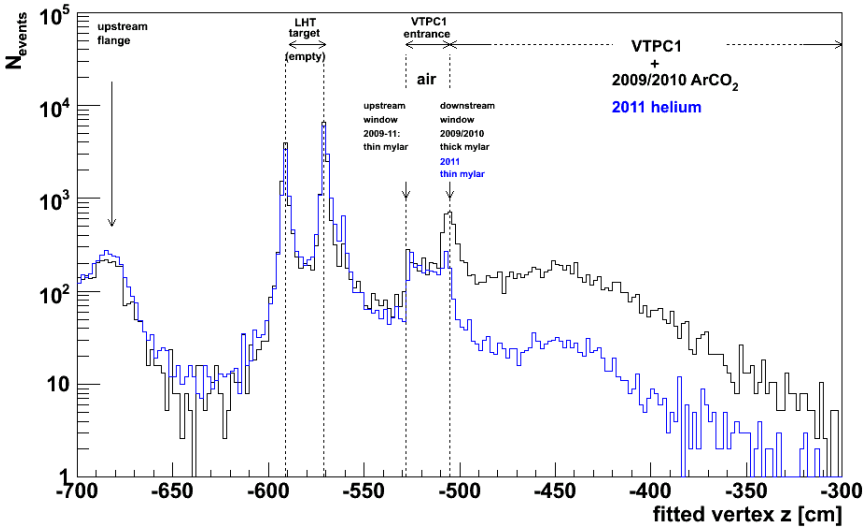

Figure 8: Interaction vertex distribution along the beam axis (data from $p+p$ interactions at 158 GeV/c) before the He beam pipe installation (2009 and 2010 data) and with the He beam pipe installed and filled with helium gas (2011 data).

of purge (Fig. 7 right) and remained constant at this level. The measured level of oxygen impurity after gas stabilization in the VTPCs was the same as that observed during the normal operation before the installation of the He beam pipes.

Figure 8 shows the interaction vertex distribution along the beam axis (data for $p+p$ interactions at 158 GeV/c) before the He beam pipe installation (2009 and 2010 data) and with the He beam pipe installed and filled with helium gas (2011 data). Clearly, the He beam pipe reduces the number of background interactions in the volume of the VTPCs by about a factor of 10.

3 The 2010 test of secondary ion beams

A 14-day long test of secondary light ion beams was performed in the H2 beam line of the CERN SPS in November/December 2010. The test marked the beginning of a new fixed target ion program at CERN. The previous one ended in 2002/2003 by runs of NA49 and NA60 with Pb and In beams, respectively.

During the test a fragment separator scheme was successfully used to produce secondary light ion beams, so far with highest momentum per nucleon of 80 GeV/c. For the first time a primary Pb beam of momentum as low as 13.9 GeV/c per nucleon was accelerated in the SPS and extracted onto the T2 target in the North Area.

The test results indicate that the properties of the secondary beam are sufficient to reach the basic physics goals of NA61. Furthermore, the test allowed to identify improvements of the primary beam and fragment separator parameters as well as of the H2 beam line and NA61 instrumentation which are necessary to reach the required performance.

The expected physics performance of NA61 with ^{7}Be and ^{11}C beams was compared, and it was concluded that the beryllium beam is preferred for the 2011 physics run.

A detailed description of the secondary light ion beam test is given in the dedicated status report submitted to the SPSC in January 2011 [5].

4 The 2011 beam period

In 2011 the NA61 beam time consists of four periods, namely: two test runs in May/June and September/October, a physics run with proton beams in July–September and a physics run with secondary Be beams in November/December. These periods are discussed below.

4.1 The test run in the SPS H2 beam line

A test run of the full NA61 detector was scheduled from May 31 to June 10, 2011. Due to malfunctioning of the North Area TAXES the run was canceled. Thus, several test and calibration activities scheduled for this run had to be shifted to the physics run with proton beams, see Sec. 4.3.

4.2 The test run in the PS T10 beam line

A test run in the T10 beam line of the PS took place from September 26 to October 10, 2011. First, tests of the the new A-detector and its time resolution were performed using leading edge discriminators (standard approach). Second, the possibility to use the 12 bits wave-form amplitude analyzer for the time measurements was tested. It was found that the time resolution of the A-detector is significantly improved when the new advanced 5 GS/s Switched Capacitor ADCs for the readout of the signals is implemented. This test is also important for a future upgrade of the NA61 ToF readout system. At present, the

data from the T10 test run are being analyzed. Preliminary results show that the time resolution of the A-detector is well below 100 ps.

4.3 The physics run with proton beams

The physics run was scheduled from July 29 to September 24, 2011. Data for two reactions were recorded:

- $p + p$ at 13 GeV/c, about 1 M events and
- $p + p$ at 158 GeV/c, about 14 M events.

About 10% of the events were recorded with non-physics triggers for data quality control and background calculations.

During the run PSD calibration data were recorded parasitically and the Z-detectors were tested. More details on these activities are given in Sec. 2.1 on detector upgrades.

At the end of the run test data taking for p + Pb interactions at 158 GeV/c took place. This included the LMPD detector which is planned to be used in the 2012 physics run for p + Pb interactions. Details are presented in Sec. 2.4.

The 2011 proton run history is presented in Fig. 9, where the number of registered events is shown as a function of time. With decreasing beam momentum the fraction of protons in the beam decreases, the beam size increases and the beam stability degrades. As a result, as seen in Fig. 9, the data taking rate at 13 GeV/c is significantly lower than one at 158 GeV/c.

5 Software upgrades

During the last year work on the new NA61 software was started. Also, significant progress was achieved on the virtualization of the software. Furthermore, the currently used software inherited from NA49 (referred here as the "old" software) was improved. These activities are briefly presented below.

5.1 The "old" software upgrades

The existing software chain was fully migrated to the default CERN operating system – SLC5 – and has been routinely used to process raw data and to perform MC simulations. The "old" software was also significantly improved via bug fixes and corrections introduced in the source code by the Shine Software development team. The CERN-supported NA61 SVN repository is a major tool for the software development within the collaboration. Several new SVN projects have started recently.

Significant progress has been made on the NA61 data base implementation. The NA61 data base is divided into two subsystems:

- the SQL-based system,

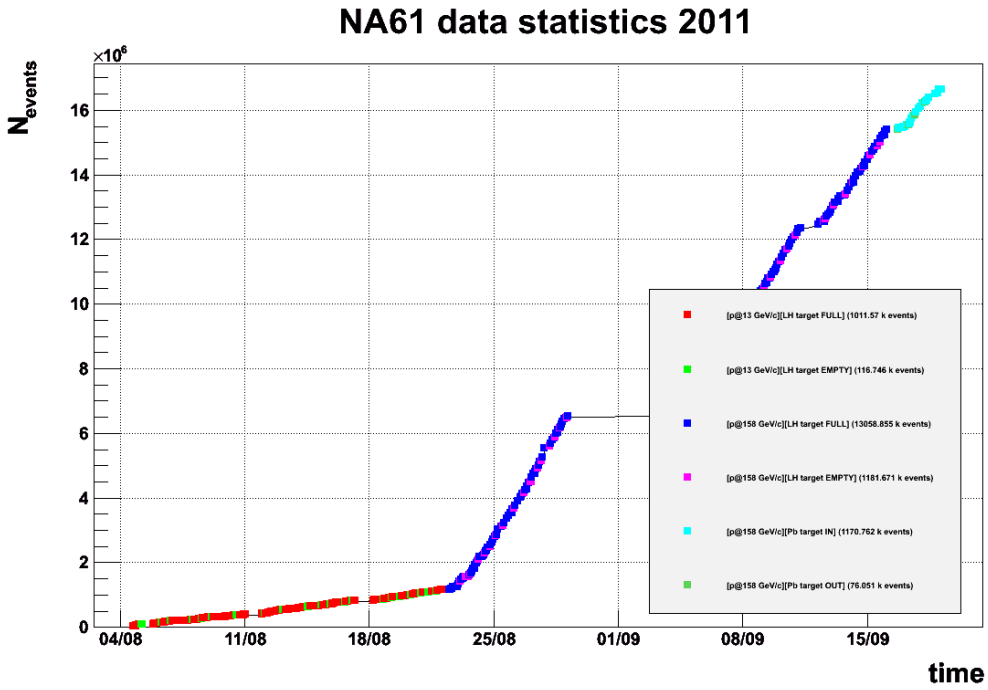

Figure 9: Number of events registered in the 2011 physics run with proton beams as a function of time.

- the DSPACK system – the data handling package, which has parameters stored in separated files.

A query from the NA61 software is sent to SQL by a plug-in of the DSPACK system. The SQL data base returns the path and file-name which is then used by the DSPACK system. In 2011 an essential update of the NA61 data base system was performed. The aim of this upgrade was to provide a simple, clean and consistent environment to store all constants and parameters. Moreover, it was necessary to add some new structures to the DB. The major updates of the DB are:

- the DSPACK part was transferred to the NA61 AFS directory,
- the cache directory was moved from a common place, which caused access problems for users, to a user-dependent private directory.
- for the CERN cluster and batch system ($LXPLUS/LXBATCH$) the cache system was removed,
- the SQL part based on MySQL Database Management System (DBMS) was moved to SQLite DBMS and located in the NA61 AFS directory,
- synchronization with the CERN VM (virtual machine) system was configured,
- reconfiguration of the plug-in system in DSPACK was done and

- the DB files were synchronized with the NA61 SVN directory.

5.2 The Shine Software development

Due to the difficulties faced concerning the maintenance and further development of the legacy NA49 software framework, a strategy for an upgrade of the offline software, in particular the reconstruction chain, was proposed in 2010. For details see the upgrade proposal and related materials [16, 17]. The key idea is to port the legacy multi-language, multi-process reconstruction chain to a single process C++ code, with a significant reuse of the working parts of the legacy chain. The C++ framework was envisaged to be based on the *Offline* software of the Pierre Auger Observatory [18]. The proposal was recommended by the CERN PH–SFT group in February 2011 [19]. Along with this, the CERN directorate provided 1 year financial support for two student (Roland Sipos and Oskar Wyszynski) working on the project at CERN.

The upgrade campaign started in March 2011 with a two-month coding workshop of the core Shine Software development group involving eight people. During this time, the following goals were achieved.

- The Auger framework was ported to the NA61 repository, parts that are irrelevant to NA61 were removed and the framework is now the backbone of the new NA61/SHINE offline framework. Moreover, the Auger installation manager for external packages was imported and adapted to the needs of NA61.

- The DSPACK memory managing system was imported to the framework to be able to interface with the parts of the legacy chain.

- The philosophy of the legacy reconstruction chain was simplified and unused components were removed. Basic validation tools were developed.

- Wrappers were designed to allow to run the old reconstruction clients as modules in the XML-based sequence of the new framework.

- The basic layout of the new event data model was designed and the new detector interface was written.

- Interfaces were written to be able to initialize the legacy processing modules within the new framework.

- An automatic code integrity verification was set up using the build-bots provided by SFT.

Following the initial setting up of the core framework the legacy C and PGI-FORTRAN processing modules were ported to the the new framework. This process finished in July 2011, and the debugging phase of these modules was carried out in August and September

2011. The validation of the performance of the legacy modules within the new framework and the legacy framework began subsequently, and is still ongoing. Meanwhile, new processing modules are being written for reconstruction of the data for new detectors.

The part of the framework for data analysis, including event visualization, DST ROOT files and simple analysis programs, was first released in September 2011 and is now being used by the collaboration.

5.3 The software virtualization

Currently, the reconstruction and analysis of NA61 and NA49 data is performed on *LXPLUS/LXBATCH*. An effort is under way to adapt the processing chain to *virtual machines* (VMs) based on *CERNVM*. A small test-*cloud* of VMs was set up at *CERN*, and CERN *IT* is in the process of building up a new cloud service, *LXCLOUD*.

CERNVM is a dedicated Linux-distribution for VMs. Although CERNVM will be constantly updated, the past versions will still be available in order to support legacy versions of the analysis software. The analysis software is distributed to the CERNVM instances via *CVMFS*, a *HTTP*-based file system for distributing pre-compiled binaries. Several versions of the analysis software can be distributed in parallel, allowing for easy reversion to older versions if needed, *e.g.* in case of problems or for comparing the results.

Since CVMFS is based on HTTP, it allows for global distribution of the software. This means processing is not restricted to CERN, but can be performed at any site running CERNVM, or having installed the CVMFS client on the physical processing nodes. CERNVM is also a step into cloud computing. It can be run on any private or public cloud supporting the *Amazon EC2* interface. The test-cloud at CERN is intended as a reference design that can easily be replicated at other sites that wish to set up a cloud. *KVM/QEMU* is used as hypervisor, and *OpenNebula* with EC2 interface is used for deploying and managing the VMs. Work is in progress to create a graphical web interface via which a user can select versions of software/VM, number of VMs and configuration for them, as well as the type of processing, and which data to process.

The NA61 software does not have to be modified to run on CERNVM. However, some changes in the processing scripts are needed, as CERNVM uses *Condor* as batch system, rather than *PBS* used by LXPLUS/LXBATCH. The complete NA61 software is available, while the NA49 software is in the process of being made available.

6 Calibration and Analysis

The progress in data calibration and analysis is briefly reported in this section.

6.1 Calibration

The calibration procedure for the 2007 data was essentially based on the approach developed for NA49. The larger amount of data collected in 2009 imposes higher requirements

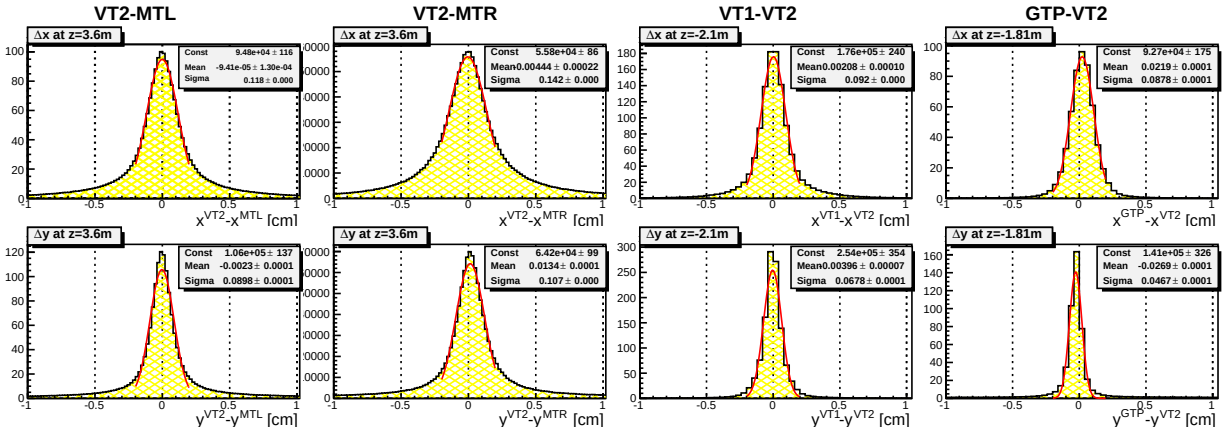

Figure 10: Calibrated 2009 data. The relative alignment of TPCs with respect to each other. Residuals of track segments extrapolated to the z-position between neighboring TPCs are shown.

on the calibration quality. In particular the assumption that various calibration parameters stay constant for a long period (assumed for 2007) can not be applied any more. Precise evaluation of the data requires time-dependent corrections.

The procedure consists of several consecutive steps resulting first in optimized parameters for the detector geometry, drift velocity and magnetic field and in a second step the calibration of the time-of-fight detectors and the energy loss in TPCs. By now calibration steps related to the track reconstruction quality of the spectrometer have been completed for all periods of the 2009 data-taking. They are:

TPC: t_0-offset corrections; corrections of $v_{\rm dr}$ as function of pressure, temperature and HV; calibration of the magnetic field scale; corrections for local distortions caused by electrostatic effects

BPD: calibration and alignment of the beam telescope detectors and their relative alignment with respect to the TPCs

Special attention was given to the calibration of the so-called Gap TPC (GPC). The GPC plays a key role in the analysis of forward produced particles. The coverage of this kinematic range is important for instance for the muon monitor measurements in T2K. Contrary to the large TPCs, the drift velocity of the GPC was not measured by the gas control system. This makes the procedure of calibration more complicated and is the reason why the GPC information was not used for the published analysis of the 2007 data. In the current procedure the calibration/alignment of the GPC is the last step. Extrapolation of tracks reconstructed in other TPCs is used to determine the GPC calibration parameters.

The achieved calibration quality is demonstrated in Fig. 10. It shows the relative alignment of the TPCs with respect to each other. Segments of a track reconstructed in different TPCs were extrapolated to the z position of the center between those TPCs and the difference of transverse coordinates x and y was plotted. One can see that residuals

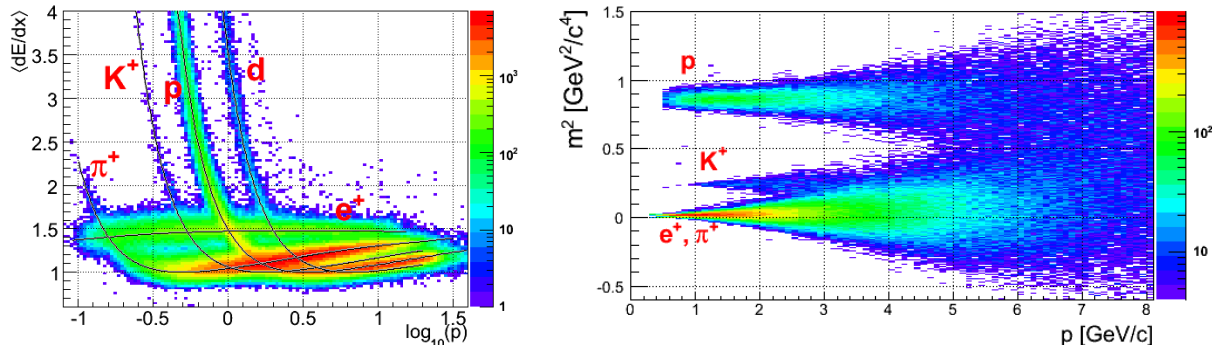

Figure 11: *Left:* Energy loss in the TPCs for positively charged particles as a function of momentum. *Right:* Mass squared derived from the ToF measurements versus momentum.

are well centered with respect to zero while mistakes in the calibration of v_{dr} would result in a bias.

The work on calibration of the PID components of the spectrometer is ongoing. Presently the first period of 2009 data-taking (p + C at 31 GeV) is fully calibrated. In Fig. 11 the energy loss distribution in the TPCs and the mass squared distribution from time-of-flight measurements are shown as a function of particle momentum. The combined $\mathrm{d}E/\mathrm{d}x$ and m^2 analysis allows to extract yields of identified particles in the cross-over region of the Bethe-Bloch curves.

In general the calibration procedure is now well established and we plan to complete the calibration of all 2009 data-taking periods by the end of autumn 2011.

6.2 Analysis of data for T2K and cosmic-ray physics

As a first priority, the cross-sections for producing charged pions from 31 GeV/c protons on carbon were measured with the thin-target data taken in 2007. The corresponding NA61/SHINE physics paper has been recently published [8]. The systematic errors are typically in the range of 5 to 10% and smaller than the statistical errors. These data (see for illustration Fig. 12) have already been used for an improved prediction of the neutrino flux in the T2K neutrino oscillation experiment [9]. Furthermore, they also provide important input to improve the hadron production models (e.g. UrQMD [12] and Fritiof [13]) needed for the interpretation of air showers initiated by ultra-high-energy cosmic rays.

The first NA61/SHINE measurements provide only one important part of what is needed to predict the neutrino flux in T2K. A substantial fraction of the high-energy flux, and in particular the electron neutrino contamination, originates from the decays of kaons. Charged kaons are readily identified in NA61/SHINE from the suite of particle identification techniques – $\mathrm{d}E/\mathrm{d}x$ in the TPCs and ToF in the upgraded detector, see Fig. 13. Recently first spectra of positively charged kaons as a function of laboratory momentum in two intervals of the laboratory polar angle covering the range from 20 up to 240 mrad were obtained. These results are summarized in Table 2.

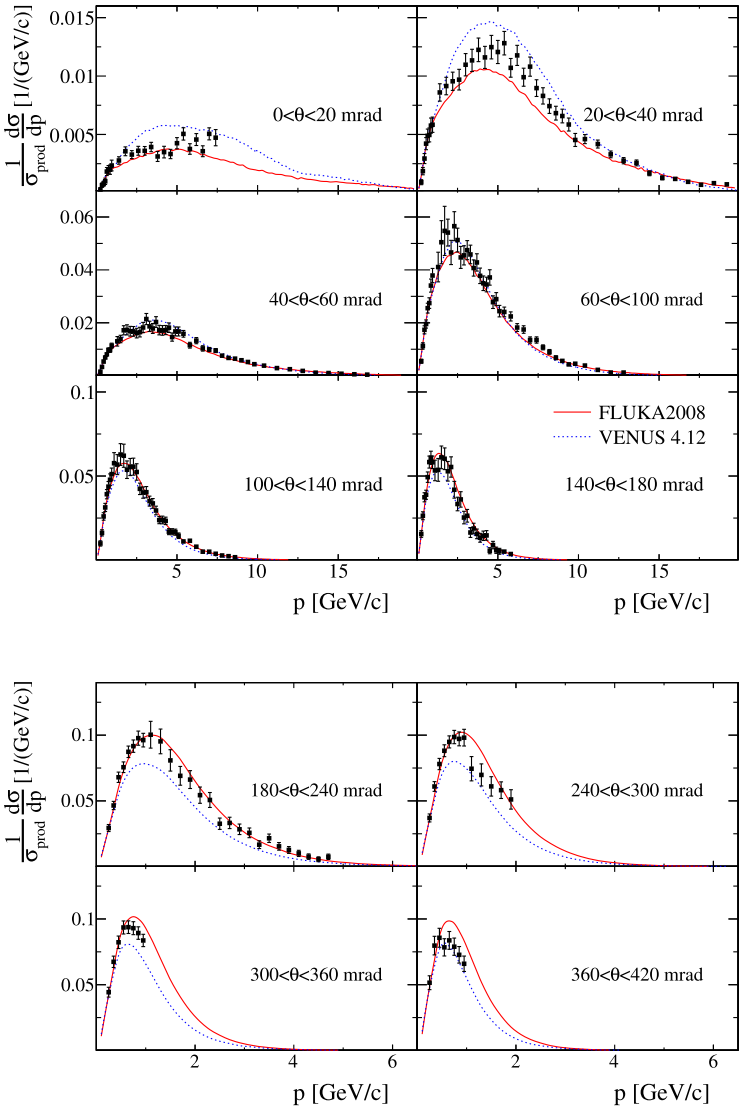

Figure 12: Laboratory momentum distributions of π^+ mesons produced in production $p + \mathrm{C}$ interactions at 31 GeV/c in different intervals of polar angle (θ). The spectra are normalized to the mean π^+ multiplicity in all production $p + \mathrm{C}$ interactions. Error bars indicate statistical and systematic uncertainties added in quadrature. The overall uncertainty (2.3%) due to the normalization procedure is not shown. Predictions of hadron production models, FLUKA2008 [10] (solid line), and Venus4.12 [11] (dotted line) are also indicated.

Also, K^+/π^+ ratios were computed using the published pion results and are shown in Fig. 14.

A large fraction (up to 40%) of the neutrinos originates from particles produced by re-interactions of secondary particles in the target, which for T2K is 90 cm long. This contribution is difficult to calculate precisely and thus motivates a careful analysis of the

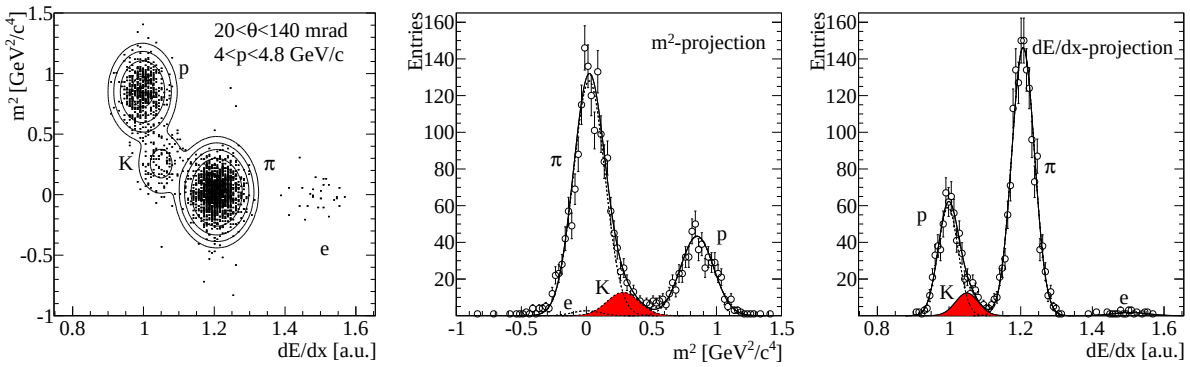

Figure 13: Example of a bi-dimensional fit to the $\mathrm{d}E/\mathrm{d}x$-m^2 distribution. The four contour lines correspond to the 1-σ and the 2-σ levels calculated from the proton (the two innermost) and the kaon (the two outermost) distribution functions. The individual m^2 and $\mathrm{d}E/\mathrm{d}x$ distributions are also shown superimposed with the results of the fitted functions.

θ_{low} (mrad)	θ_{high} (mrad)	p_{low} (GeV/c)	p_{high} (GeV/c)	N_K	$\mathrm{d}\sigma^{k^+}/\mathrm{d}p$ (mb/(GeV/c))	Δ_{stat}	Δ_{sys}
20	140	1.6	2.4	56	2	0.27	0.08
		2.4	3.2	106	2.33	0.22	0.09
		3.2	4	134	2.46	0.22	0.09
		4	4.8	127	2.16	0.21	0.09
		4.8	5.6	126	1.99	0.19	0.07
		5.6	6.4	97	1.51	0.17	0.05
		6.4	7.2	81	1.19	0.18	0.09
140	240	1.6	2.4	49	3	0.41	0.11
		2.4	4	64	1.4	0.17	0.06
		4	5.6	32	0.56	0.1	0.06

Table 2: The NA61/SHINE preliminary results on the differential K^+ production cross section in the laboratory system, $\mathrm{d}\sigma/\mathrm{d}p$, for $p+\mathrm{C}$ interactions at 31 GeV/c. Each row refers to a different ($p_{\mathrm{low}} \leq p \leq p_{\mathrm{up}}, \theta_{\mathrm{low}} \leq \theta < \theta_{\mathrm{up}}$) bin, where p and θ are the kaon momentum and polar angle in the laboratory frame. N_K is the fitted raw number of kaons. The central value as well as the statistical (Δ_{stat}) and systematic (Δ_{sys}) errors of the cross section are given. The overall uncertainty (2.5%) due to the normalization procedure is not included.

data taken with the long target. Pilot NA61 results were presented at the NUFACT meeting held at CERN at the beginning of August [14]. The ultimate precision will come from the analysis of the long-target data taken in 2010. Work is ongoing to obtain results

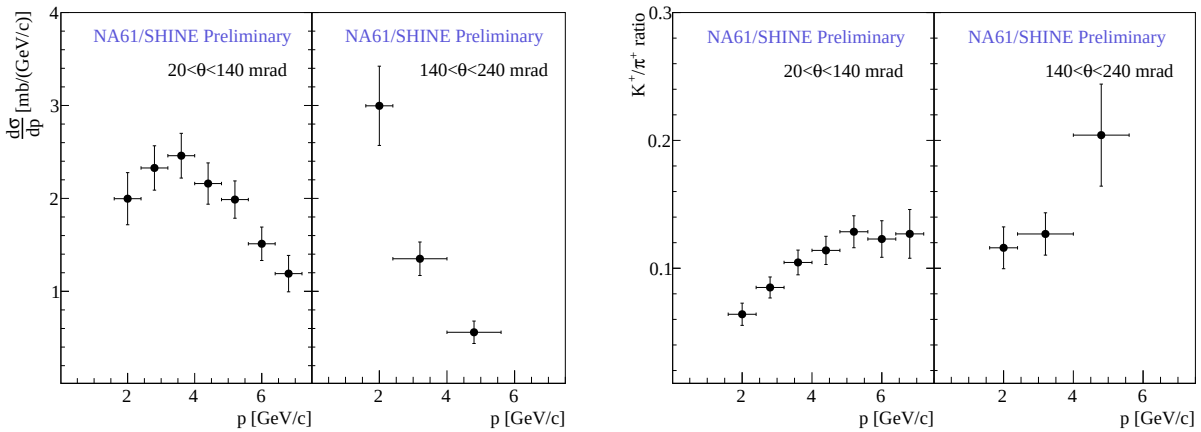

Figure 14: *Left:* Differential cross sections for K^+ production in $p + \mathrm{C}$ interactions at $31\,\mathrm{GeV}/c$. The spectra are presented as a function of laboratory momentum, p, in two different intervals of polar angle, θ. Error bars indicate statistical and systematic uncertainties added in quadrature. The overall uncertainty (2.5%) due to the normalization procedure is not included. *Right:* Ratio of K^+ over π^+ production in $p + \mathrm{C}$ interactions at $31\,\mathrm{GeV}/c$. The spectra are presented as a function of laboratory momentum p in two different intervals of polar angle θ. Errors are calculated taking into account only statistical uncertainties.

in time for the high-statistics measurements that will become possible in T2K when the experiment resumes data taking after recovering from damage in the massive earthquake in north-eastern Japan that occurred in March 2011.

In addition to the $31\,\mathrm{GeV}/c$ data set, pion on carbon data was collected in 2009 at beam energies of 158 and $350\,\mathrm{GeV}/c$ for the purpose of improving the interpretation of ultra-high energy cosmic ray air shower observations. As can be seen in Fig. 15, the measured spectra cover a large region of phase space with good statistical accuracy. This data set will also provide measurements of strange particle yields in π^-+C reactions for the first time that will allow a tuning of the string fragmentation parameters of hadronic event generators used in cosmic ray physics, see Fig. 15 right.

6.3 Analysis for ion physics

Preliminary results on m_T and rapidity spectra of negatively charged pions and K^0_S were obtained in $p + \mathrm{C}$ interactions at $31\,\mathrm{GeV}/c$ (see Figs. 16 and 17). The negative pion spectra were extracted with the so-called h^- method where all negatively charged hadrons produced in the collisions are assumed to be pions and the small contribution of other particle types is subtracted using simulations.

The rapidity and transverse mass spectra of π^- mesons at mid-rapidity are shown in Fig. 16 and compared to NA49 results for central Pb+Pb collisions at $30A\,\mathrm{GeV}/c$ [21]. The

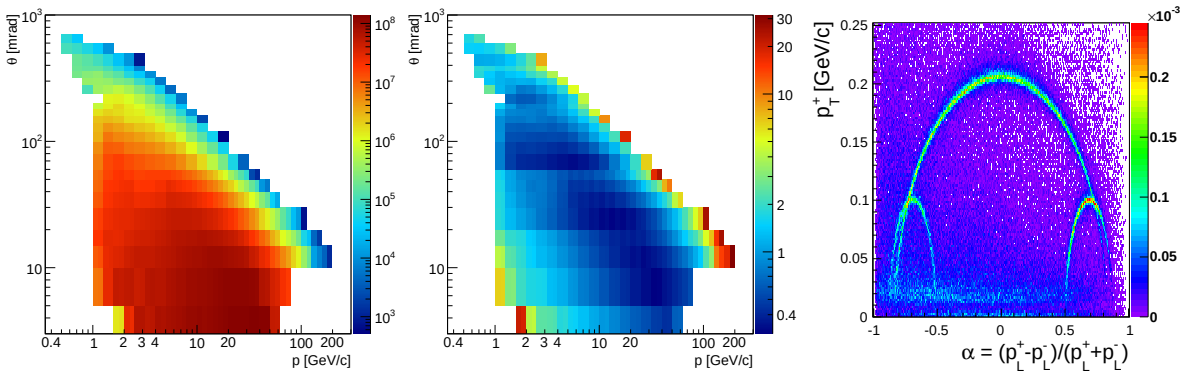

Figure 15: *Left:* Number of negatively charged tracks in π^-+C interactions at 350 GeV/c after fiducial cuts and quality selection. The color scale denotes events per GeV/c per steradian. *Middle:* Relative statistical uncertainty in percent of the spectra shown on the left panel. *Right:* Armenteros-Podolansky plot after application of the V_0 selection cuts.

Pb+Pb rapidity spectrum was divided by the mean number of wounded nucleons from the projectile nucleus (the mean pion multiplicity in the forward hemisphere is approximately proportional to the mean number of wounded nucleons of the projectile nucleus). The shape of the m_{T} spectrum at mid-rapidity changes from a convex form in $p+\mathrm{C}$ to a concave one in central Pb + Pb interactions. According to the hydrodynamical approach this is due to the strong radial collective flow in Pb + Pb collisions, which is absent in $p+\mathrm{C}$ interactions. Inverse slope parameters of transverse mass spectra were calculated for $0.2 < m_{\mathrm{T}} - m_{\pi} < 0.7\,\mathrm{GeV}/c^2$. They increase from $T = 151 \pm 3\,\mathrm{MeV}/c$ for $p+\mathrm{C}$ at 31 GeV/c to $T = 157 \pm 2\,\mathrm{MeV}/c$ for Pb + Pb at 30A GeV/c [23].

The analysis of resonance production started. First results on Δ^{++} production in $p+\mathrm{C}$ interactions at 31 GeV/c are shown in Fig. 18. The combinatorial background was calculated by the mixing method, which is currently being optimized.

Methods and software needed for analysis of data on $p+p$ interactions were further developed. Currently all the necessary programs to study spectra, yields and event-by-event fluctuations are ready. In the case of $p+p$ collisions a significant fraction of recorded events are non-target interactions (with windows of the liquid hydrogen target, TPC gas, etc.). In order to correct the results for this contamination approximately 10% of events were recorded with an empty liquid hydrogen target. The methods of normalization and subtraction for spectra, yields and event-by-event fluctuations were tested using uncalibrated 2009 $p+p$ data [15, 20].

Preliminary results on event-by-event average p_{T} and multiplicity fluctuations (not shown here) were obtained via the $\Phi_{p_{\mathrm{T}}}$ measure [24] and the scaled variance ω of the multiplicity distribution [25], respectively.

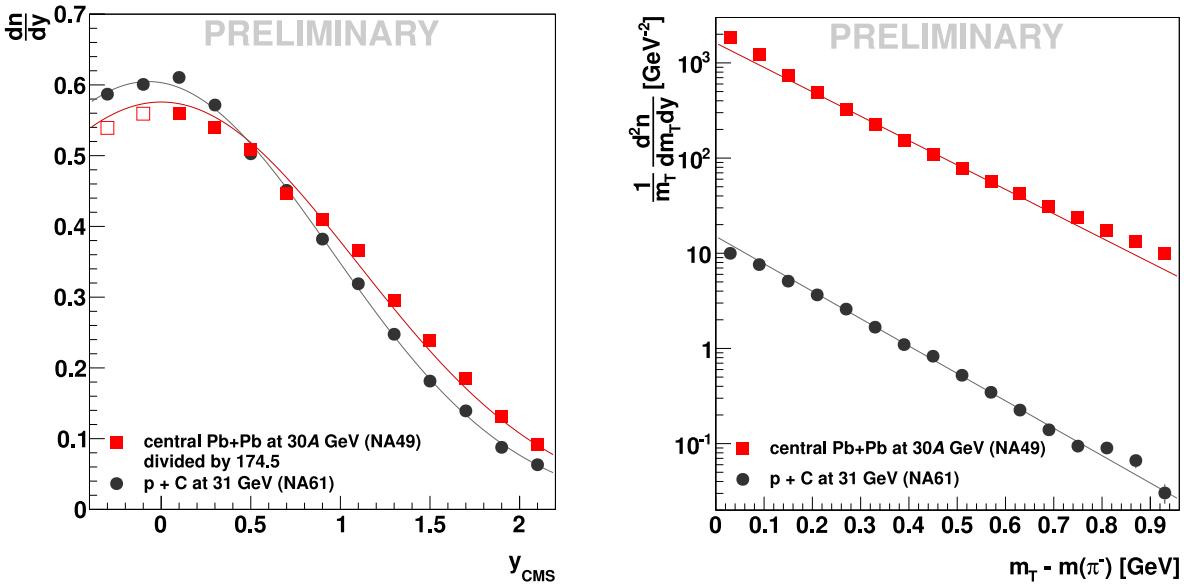

Figure 16: Rapidity (left) and transverse mass spectra at mid-rapidity (right) of π^- produced in p + C interactions at 31 GeV/c and 7.2% most central Pb + Pb collisions at 30A GeV. Taken from [22, 23].

7 Recent LHC and RHIC results and the NA49 evidence for the onset of deconfinement

In August 2011 the NA61/SHINE Collaboration submitted to the SPSC a memorandum [6] which reports on the status of the evidence for the onset of deconfinement in central Pb+Pb collisions at low SPS energies and underlines the urgent need for a timely execution of the NA61/SHINE ion program. Recent results from the RHIC beam energy scan program agree with NA49 measurements in the region of the onset of deconfinement. The new LHC data confirm the interpretation of the structures observed at low SPS energies as due to the onset of deconfinement. The four representative plots are shown in Fig. 19. They present the experimental results available in mid-2011.

Thus the physics justification of the NA61/SHINE ion program, the observation of the onset of deconfinement at the low SPS energies, is strongly confirmed by independent measurements. These recent developments underline the urgency of carrying out the NA61/SHINE ion program as soon as technically possible. In particular, the most urgent data for this program, central Ar + Ca collisions at 13A, 20A, 30A, 40A, 80A and 158A GeV/c should be taken with as little delay as possible. It is also crucial to complete the energy scan with secondary Be beams in 2011 and 2012.

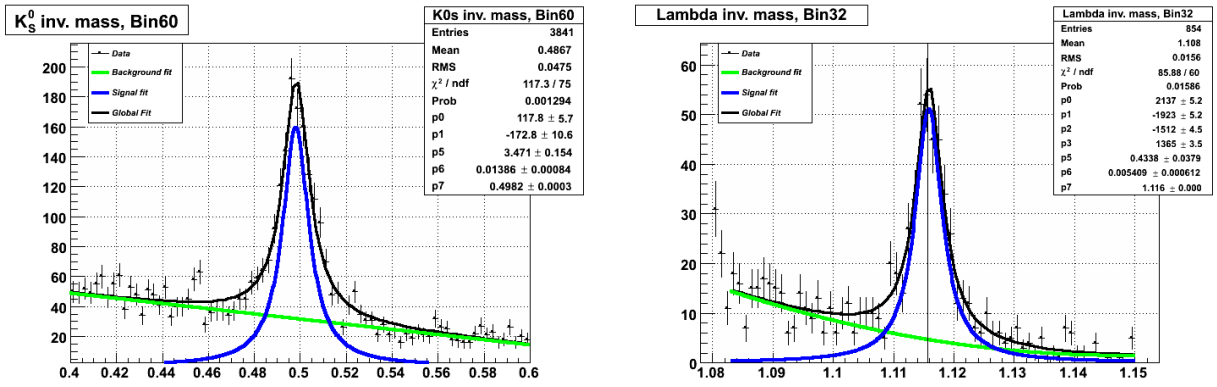

Figure 17: Example of invariant mass distributions close to K^0_S peak in the interval $p_{\mathrm{T}} < 0.2\,\mathrm{GeV}/c$ and $1 < y < 1.5$ (left) and close to Λ peak in the interval $0.4 < p_{\mathrm{T}} < 0.6\,\mathrm{GeV}/c$ and $-1.25 < y < 1$ (right).

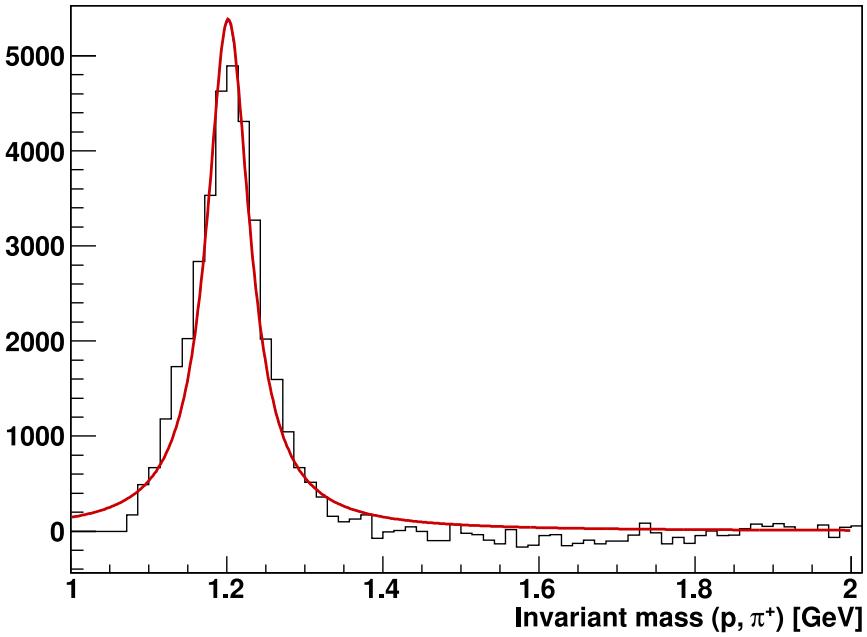

Figure 18: Invariant mass of p and π^+ showing the $\Delta^{++} \to p\pi^+$ resonance state. Mass identification was based on energy loss measurements in the TPCs and time of flight from ToF detectors.

8 Data taking plans

The data taking schedule presented in the 2010 Annual Report [15] has to be modified due to a shift of the accelerator stop from 2012 to 2013. The revised NA61/SHINE data taking plan is presented in Table 3.

The most dramatic change compared to the data taking plan proposed in 2010 [15] is

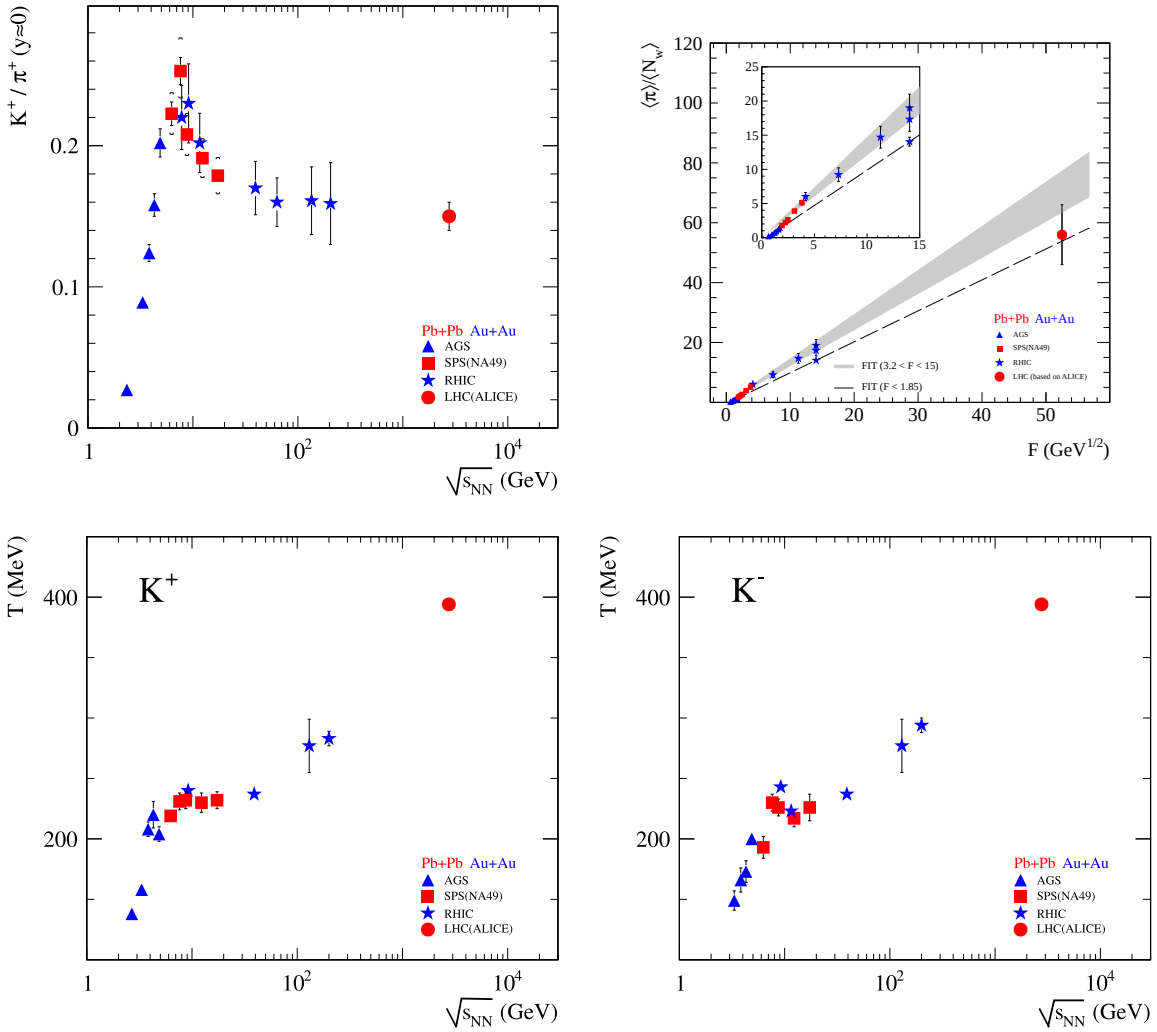

Figure 19: Heating curves of strongly interacting matter, status mid-2011. Hadron production properties (see Ref. [7] for details) are plotted as a function of collision energy ($\sqrt{s_{NN}}$ and $F \approx \sqrt{\sqrt{s_{NN}}}$) for central Pb + Pb (Au + Au) collisions: top-left – the K^+/π^+ ratio, top-right – the mean pion multiplicity per participant nucleon, bottom-left – the inverse slope parameter of the transverse mass spectra of K^+ mesons and bottom-right – the inverse slope parameter of the transverse mass spectra of K^- mesons. The observed changes of the energy dependence for central Pb + Pb (Au + Au) collisions are related to: decrease of the mass of strangeness carriers and the ratio of strange to non-strange degrees of freedom (*horn*: top-left plot), increase of entropy production (*kink*: top-right plot), weakening of transverse expansion at the onset of deconfinement (*step*: bottom plots).

a shift of the run with Ar beams from 2013 to 2014. Data taking with Ar beams has the highest physics priority. It was originally recommended by the SPSC to take place in 2009 and was subsequently shifted to 2012 and 2013 to achieve compatibility with the changing LHC schedule. Further delay of the run with Ar beams and consequently the longer

Beam **Primary**	**Beam** **Secondary**	**Target**	**Energy** (A GeV)	**Year**	**Days**	**Physics**
Pb			40, 80, 158			
	^{7}Be	Be	40, 80, 158	2011	3×8 days	CP, OD
Pb			13, 20, 30			
	^{7}Be	Be	13, 20, 30	2012	3×12 days	CP, OD
p			400			
	p	Pb	158	2012	60 days	High p_{T}
Ar		Ca	13, 20, 30, 40, 80, 158	2014	6×8 days	CP, OD
p			400			
	p	Pb	13, 20, 30, 40, 80, 158	2014	6×7 days	CP, OD
Xe		La	13, 20, 30, 40, 80, 158	2015	6×8 days	CP, OD

Table 3: The NA61/SHINE data taking plan revised due to the 2013 accelerator stop. The runs with secondary ^{7}Be beams are planned for 2011 and 2012, whereas primary ion beams are planned to be used in 2014 and 2015. The following abbreviations are used for the physics goals of the data taking: CP – Critical Point, OD – Onset of Deconfinement.

duration of the whole ion program has a strong negative impact on NA61. In particular questions of manpower, finances and detector stability over the extended period should be solved. The probability of a successful completion of the whole program is endangered.

It is therefore of key importance to ensure that the run with Ar beams will take place in 2014 without further delay. Ar and Xe beams are possible in 2014 and 2015 provided the ion source and the Linac are operational for 26 weeks in 2013 [26]. This request still needs approval by the CERN authorities.

Clearly for proper completion of the whole program sufficient beam time for the Be run in 2012 and for the Xe run in 2015 is required as indicated in Table 3. There is a possibility to start the 2012 Be run at the beginning of September 2012 instead of November 2012 [26]. This may help to better accommodate the needs of other fixed target experiments. NA61 is ready to take the Be beam anytime in 2012.

Finally we note that a discussion has started at RHIC on the possibility of a beam energy scan with medium size ions and data taking in the fixed target mode.

9 Appendix: NA61 publications and conference contributions October 2010 – September 2011

1. Measurements of Cross Sections and Charged Pion Spectra in Proton-Carbon Interactions at 31 GeV/c,
   N. Abgrall *et al.* [NA61/SHINE Collaboration],
   Phys. Rev. **C84**, 034604 (2011). [arXiv:1102.0983 [hep-ex]].

2. Pion production in 30 GeV $p + \mathrm{C}$: First results from NA61/SHINE,
   S. Murphy et al.,
   NUFACT10 Tata Institute, Mumbai 20–25 October, 2010

3. NA61 status and plans,
   M. Slodkowski et al.,
   6th ICPAQGP2010 6–10 December 2010 at Goa, India

4. Measurements of Cross Sections and Charged Pion Spectra in Proton Carbon Interactions at 31 GeV/c,
   L. Esposito et al.,
   WIN'11 International Workshop on WEAK INTERACTIONS AND NEUTRINOS

5. Pion production in 30 GeV $p + \mathrm{C}$: First results from NA61/SHINE,
   S. Murphy et al.,
   MORIOND EW Interactions and Unified Theories March 13th – 20th, 2011

6. Results from Hadroproduction Experiments,
   B. Popov et al.,
   Neutrino Telescopes in Venice 15–18 March, 2011

7. NA49/NA61: results and plans on beam energy and system size scan,
   M. Gazdzicki et al.,
   Quark Matter 2011, Annecy, France

8. Projectile Spectator Detector for the heavy ion program of the NA61/SHINE experiment at the CERN SPS,
   A. Kurepin et al.,
   Quark Matter 2011, Annecy, France

9. Pion production in $p + \mathrm{C}$ collisions at 31 GeV/c,
   A. Aduszkiewicz and T. Palczewski et al.,
   Quark Matter 2011, Annecy, France

10. Hadron calorimeter with MAPD readout in the NA61/SHINE experiment,
    A. Ivashkin et al.,
    New Developments in Photodetection, Lyon, France, 4–8 July 2011

11. Measurement of charged pion and kaon production in proton-carbon interaction at 31 GeV/c from NA61/SHINE,
A. Korzenev et al.,
The 2011 Europhysics Conference on High Energy Physics 21–27 July 2011, Grenoble, Rhône-Alpes France

12. NA61/SHINE experiment: ion program,
R. Planeta et al.,
The 2011 Europhysics Conference on High Energy Physics 21–27 July 2011, Grenoble, Rhône-Alpes France

13. Critical Point and Onset of Deconfinement - NA61/SHINE Ion Program,
G. Stefanek et al.,
PANIC 2011, MIT USA

14. Hadron Production Measurement in NA61/SHINE Experiment at CERN SPS for the Neutrino and Cosmic Ray Experiments,
T. Palczewski et al.,
PANIC 2011, MIT USA

15. Measurements of Cross Sections and Charged Pion Spectra in Proton-Carbon Interactions at 31 GeV/c,
M. Posiadala et al.,
NUFACT11, 1–6 August 2011, Geneve

16. Strange Particle Measurements with the NA61 experiment,
S. di Luise et al.,
NUFACT11, 1–6 August 2011, Geneve

17. The NA61/SHINE long target pilot analysis for T2K,
N. Abgrall et al.,
NUFACT11, 1–6 August 2011, Geneve

18. Hadroproduction Measurements with NA61/SHINE for the Understanding of Extensive Air Showers,
M. Unger et al.,
Int. Cosmic Ray Conference (ICRC 2011), August 2011, Beijing, China

19. Eksperyment NA61/SHINE przy akceleratorze SPS w CERN-ie,
R. Planeta et al.,
XLI Zjazd Fizykow Polskich, Lublin, September 2011

20. The NA61/SHINE hadron production experiment for T2K: update and recent results,
S. Murphy et al.,
TAUP 2011 5 – 9 September 2011, Munich, Germany

21. NA61/SHINE at the CERN SPS: plans, status and first results,
A. Aduszkiewicz et al.,
Strangness in Quark Matter Conference, Krakow, Poland, September 2011

22. The NA61/SHINE Physics Program – first results and future plans,
T. Czopowicz et al.,
ISMD2011, Hiroshima, Japan, September 2011

Acknowledgments: We would like to thanks the CERN PH, BE and EN Departments for the strong support of NA61. We are very grateful to Joachim Baechler, Ilia Krasin and Martin Wensveen for their contribution to the He beam pipe and LMPD upgrades.

This work was supported by the Hungarian Scientific Research Fund (grants OTKA 68506 and 79840, OTKA/NFU A08-77719 and A08-77815), the Bolyai Scholarship of the Hungarian Academy of Sciences, the Polish Ministry of Science and Higher Education (grants 667/N-CERN/2010/0 and N N202 484339), the Federal Agency of Education of the Ministry of Education and Science of the Russian Federation (grant RNP 2.2.2.2.1547), the Russian Academy of Science and the Russian Foundation for Basic Research (grants 08-02-00018 and 09-02-00664), the Ministry of Education, Culture, Sports, Science and Technology, Japan, Grant-in-Aid for Scientific Research (grants 18071005, 19034011, 19740162, 20740160 and 20039012), the German Research Foundation (grant GA 1480/2-1) Swiss Nationalfonds Foundation (grant 200020-117913/1) and ETH Research Grant TH-01 07-3.

References

[1] N. Antoniou *et al.* [NA61/SHINE Collaboration], CERN-SPSC-2006-034.

[2] Tedlar – polyvinyl fluoride (PVF) films, `http://www2.dupont.com/Tedlar`

[3] Airex foams, `http://www.airexag.ch/en`

[4] Carbon fiber Toray, `http://www.torayca.com/pdfs/M55JDataSheet.pdf`

[5] N. Abgrall *et al.*, [NA61/SHINE Collaboration], CERN-SPSC-2011-005; SPSC-SR-077, `http://cdsweb.cern.ch/record/1322135?ln=en`

[6] N. Abgrall *et al.*, [NA61/SHINE Collaboration], CERN-SPSC-2011-028; SPSC-M-775, `http://cdsweb.cern.ch/record/1377835?ln=en`

[7] M. Gazdzicki, M. Gorenstein, P. Seyboth, Acta Phys. Polon. B **42**, 307 (2011) [arXiv:1006.1765 [hep-ph]].

[8] N. Abgrall *et al.* [NA61/SHINE Collaboration], Phys. Rev. C **84** (2011) 034604; arXiv:1102.0983 [hep-ex].

[9] K. Abe *et al.* [T2K Collaboration], Phys. Rev. Lett. **107** (2011) 041801; arXiv:1106.2822 [hep-ex].

[10] A. Fasso *et al.*, Report No. CERN-2005-10, 2005; G. Battistoni *et al.*, AIP Conf. Proc. **896**, 31, (2007).

[11] K. Werner, Nucl. Phys. A **525**, 501c (1991);
Phys. Rep. **232**, 87 (1993).

[12] V. Uzhinsky, "How to Improve UrQMD Model to Describe NA61/SHINE Experimental Data", arXiv:1107.0374 [hep-ph].

[13] V. Uzhinsky, "Tuning of the GEANT4 FRITIOF (FTF) Model Using NA61/SHINE Experimental Data", arXiv:1109.6768 [hep-ph].

[14] N. Abgrall (for the NA61/SHINE Collaboration), "The NA61/SHINE long target pilot analysis for T2K", arXiv:1110.1966 [hep-ex];
N. Abgrall, Ph.D. thesis, University of Geneva, Geneva, Switzerland, 2011.

[15] N. Abgrall *et al.*, [NA61/SHINE Collaboration], CERN-SPSC-2010-025; SPSC-SR-066, `http://cdsweb.cern.ch/record/1292313?ln=en`.

[16] NA61/SHINE offline software upgrade proposal [`https://indico.cern.ch/getFile.py/access?resId=0&materialId=0&confId=125760`].

[17] NA61/SHINE offline software upgrade supplementary material [https://indico.cern.ch/conferenceDisplay.py?confId=125760].

[18] S. Argiró *et al.*, "The Offline Software Framework of the Pierre Auger Observatory," Nucl. Instrum. Meth. A **580** (2007) 1485–1496.

[19] NA61/SHINE offline software upgrade proposal review by CERN PH-SFT [https://indico.cern.ch/getFile.py/access?resId=1&materialId=0&confId=126464].

[20] T. Cetner and K. Grebieszkow (for the NA61 Collaboration), arXiv:1101.0710.

[21] C. Alt *et al.* [NA49 Collab.], Phys. Rev. C **77**, 024903 (2008).

[22] M. Gaździcki (for the NA49 and NA61/SHINE Collaborations), arXiv:1107.2345.

[23] A. Aduszkiewicz (for the NA61 Collaboration), talk at SQM 2011, http://indico.ujk.edu.pl/conferenceDisplay.py?confId=0

[24] M. Gaździcki and S. Mrówczyński, Z. Phys. C **54** 127 (1992).

[25] V.V. Begun *et al.*, Phys. Rev. C **70**, 034901 (2004).

[26] D. Manglunki, the SPS Light Ion Project Leader, the CERN BE Department, private communication